Communications for Statistical Applications and Methods
2013, Vol. 20, No. 1, 77–84

DOI: http://dx.doi.org/10.5351/CSAM.2013.20.1.077

Evaluation of the Efficiency of an Inverse Exponential Kernel Estimator for Spherical Data

Hyun Suk Park[1,a]

[a]Department of Finance and Information Statistics, Hallym University

Abstract

This paper deals with the relative efficiency of two kernel estimators $\hat{f}_n$ and $\hat{g}_n$ by using spherical data, as proposed by Park (2012), and Bai *et al.* (1988), respectively. For this, we suggest the computing flows for the relative efficiency on the 2-dimensional unit sphere. An evaluation procedure between two estimators (given the same kernels) is also illustrated through the observed data on normals to the orbital planes of long-period comets.

Keywords: Exponential kernel estimator, relative efficiency, orbital planes of long-period comets.

1. Introduction

Suppose that *i.i.d.* random variables $X_1, \ldots, X_n$ have a probability density function f on $\mathbb{S}^2$ with respect to dV_g, which is a volume element of associated with the Riemannian metric g. Then the kernel estimator of $f(p)$ based on $X_1, \ldots, X_n$ is of the form

$$\hat{f}_n(p) = \frac{1}{nh^2C_h} \sum_{i=1}^{n} K\left(\frac{1}{h} \exp_p^{-1} X_i\right), \quad p \in \mathbb{S}^2, \tag{1.1}$$

where C_h is the positive constant and h is the smoothing parameter such that

$$h^2C_h = \int_{\mathbb{S}^2} K\left(\frac{1}{h} \exp_p^{-1} x\right) dV_g(p). \tag{1.2}$$

The integral of (1.2) is independent of x and $C_h/\omega_1 \to 1$ as $h \to 0$, where ω_1 is an area of the surface of the unit sphere (see Section 2, Park, 2012). The kernel function in (1.1) is defined on the tangent space $T_p(\mathbb{S}^2)$ such that $\int_{T_p(\mathbb{S}^2)} K(v)dv = 1$. Usually K is taken as a radially symmetric unimodal probability function in the case of the m-dimensional Euclidean space. Hence we may choose $K(v) = T(< v, v >_p^{1/2})$ for $v \in T_p(\mathbb{S}^2)$ in the estimator (1.1), where $< \cdot, \cdot >_p$ is the inner product with respect to the metric g, such that for some constant $c > 0$ and $l = 1, 2$, as $h \to 0$,

$$\int_{\frac{c}{h}}^{\infty} T^l(y) y^{k+1} dy = o(h^\alpha), \quad \text{for } k = 1, 2, \ldots \text{ and } \alpha = 1, 2, \ldots .$$

The motive we consider the kernel estimator (1.1) is that not all procedures used in the Euclidean space can be properly translated when considering the statistical problem of estimating a density function defined on the non-Euclidean space. To solve this problem, the *exponential map* for connecting

This research was supported by the Hallym University Research Fund, 2011(HRF-201109-041).

[1] Associate Professor, Department of Finance and Information Statistics, Hallym University, 39 Hallym DaeHak-Jil, Okchun-Dong, Chuncheon 200-702, Korea. E-mail: hspark@hallym.ac.kr

the 2-dimensional unit sphere $\mathbb{S}^2$ valued random sample X_i with the argument in the kernel function defined on the tangent space $T_p(\mathbb{S}^2)$ is considered. The exponential map, $\exp_p : T_p(\mathbb{S}^2) \to \mathbb{S}^2$, is defined by $\exp_p \xi = \gamma_\xi(1)$, where $\gamma_\xi(t) = \exp_p t\xi$ is the geodesic through $p \in \mathbb{S}^2$ at $t = 0$ with $d\gamma_\xi/dt\,|_{t=0} = \xi \in T_p(\mathbb{S}^2)$. See Figure 1, p.3 in Park (2012) for more details of the exponential map.

Explicit computations of the inverse exponential map on the estimator (1.1) are as follows: For any pair (ξ_1, ξ_2) of orthonormal vectors where $\xi_1 \in \mathbb{S}^2$ and $T_{\xi_1} = \{\xi_2 \in \mathbb{S}^2 | \xi_1 \perp \xi_2\}$, we consider a curve $\gamma_\xi : T_{\xi_1} \times [0, \pi) \to \mathbb{S}^2$ given by

$$\gamma_\xi(t) = \xi_1 \cos(t) + \xi_2 \sin(t). \tag{1.3}$$

Here γ_ξ is a great circle of $\mathbb{S}^2$ passing through the points ξ_1 and ξ_2, *i.e.*, γ_ξ is a geodesic on $\mathbb{S}^2$. Then an inverse parametrization can be deduced from (1.3) for which $\gamma_\xi^{-1} : \mathbb{S}^2 \backslash \{\xi_1, -\xi_1\} \to T_{\xi_1} \times [0, \pi]$ would be an inverse exponential map. Let $p \in \mathbb{S}^2$ and $v \in T_p(\mathbb{S}^2)$ be given. It is obvious that $p \perp v$. Putting $\xi_1 = p$ and $\xi_2 = v/\|v\|$, the curve $\gamma_v(t) = p \cos \|v\|t + (v/\|v\|) \sin \|v\|t$ is the geodesic passing through p tangent to $\dot{\gamma}_v(0) = v$. Hence the exponential map of $T_p(\mathbb{S}^2) \to \mathbb{S}^2$ is given by

$$\exp_p v = p \cos \|v\| + \frac{v}{\|v\|} \sin \|v\|. \tag{1.4}$$

Here the distance from p to $\exp_p v$ is $d(p, \exp_p v) = \|v\|$. For $p \in \mathbb{S}^2$, we have $\mathcal{D}_p = \{v \in T_p(\mathbb{S}^2) : \|v\| < \pi\}$ and $\exp_p(\mathcal{D}_p) = \mathbb{S}^2 \setminus \{-p\}$, where the cut locus is reduced to the single point, $\mathrm{cut}(p) = \{-p\}$. By (1.4) and $d(p, \exp_p v) = \|v\|$, the inverse exponential map, $\exp_p^{-1} : \mathbb{S}^2 \to T_p(\mathbb{S}^2)$ is given by

$$\exp_p^{-1} x = \cos^{-1}\left(p^t x\right)\xi, \tag{1.5}$$

where ξ is an unit tangent vector orthogonal to p. Submitting (1.5) into (1.1), we obtain (1.6) and (1.7) as follows.

$$\hat{f}_n(p) = \frac{1}{nh^2 C_h} \sum_{i=1}^{n} K\left(\frac{1}{h} \cos^{-1}\left(p^t X_i\right)\xi_i\right), \tag{1.6}$$

where ξ_i is an unit tangent vector orthogonal to p, and C_h is the positive normalized constant such that

$$h^2 C_h = \int_{\mathbb{S}^2} K\left(\frac{1}{h} \cos^{-1}\left(p^t x\right)\xi\right) dV_g(p). \tag{1.7}$$

In this paper, the problem of evaluating relative efficiency between the kernel estimators is investigated. For this, we first refer to the kernel estimator in order to make an evaluation of relative efficiency as follows. Given *i.i.d.* random variables $X_1, X_2, \ldots, X_n$ with unknown density f on the 2-dimensional unit sphere $\mathbb{S}^2$, the kernel estimator of Bai *et al.* (1988) is, for a kernel function L and the smoothing parameter λ,

$$\hat{g}_n(x) = n^{-1} d_0(\lambda) \sum_{i=1}^{n} L\left(\lambda\left(1 - x^t X_i\right)\right), \tag{1.8}$$

where $d_0(\lambda)$ is selected so that $\hat{g}_n(x)$ integrates to unity. When x is close to X_i, $(1 - x^t X_i)$ is close to zero, and also $\exp_p^{-1} X_i$ is close to zero. Actually, the estimators in (1.1) and (1.8) have the same

characteristics and different kernels are not called for as note in Hall *et al.* (1987). In addition, we can check that the estimator of type (1.1) has identical first-order asymptotics (see Lemmas in Appendix).

We focus on two points in this paper. First, we aim for an evaluation of the asymptotic relative efficiency (ARE) of the kernel estimator (1.1) on 2-dimensional unit sphere as follows.

Theorem 1. *When f is 2-times differentiable, the asymptotic relative efficiency (ARE) of $\hat{g}_n$ with respect to $\hat{f}_n$ is given by*

$$ARE\left(\hat{g}_n; \hat{f}_n\right) = \frac{C_1\left(\frac{C_1}{2C_2}\right)^{-\frac{1}{3}} + C_2\left(\frac{C_1}{2C_2}\right)^{\frac{2}{3}}}{D_1\left(\frac{D_1}{2D_2}\right)^{-\frac{1}{3}} + D_2\left(\frac{D_1}{2D_2}\right)^{\frac{2}{3}}}, \tag{1.9}$$

where

$$\begin{aligned} C_1 &= \pi \int_0^\infty T^2(s) s ds, & C_2 &= \left(\frac{\pi}{4C_h}\int_0^\infty T(s)s^3 ds\right)^2 \int_{\mathbb{S}^2} (\Delta f(p))^2 dV_g(p), \\ D_1 &= \frac{\pi\lambda\alpha_2(T)}{nc(\lambda)^{-2}}, & D_2 &= \left(\int_{T_x} D_\xi^2 \overline{g_\xi}(x) d\mu_1(\xi)\right)^2 \cdot \alpha_1(T)^2, \end{aligned} \tag{1.10}$$

where $C(\lambda; T) = \sqrt{\pi}/(2!\lambda^2\alpha_0(T))$, $\alpha_0(T) = \int_0^\infty T(s)s\,ds$, $D_\xi^s g_\xi = D_\xi D_\xi^{s-1} g_\xi$, $\alpha_1(T) = \int_0^\infty T(s)s^3 ds$, $\alpha_2(T) = \int_0^\infty T(s^2)s\,ds$, $\overline{g_\xi}(x) = g_\xi(x/\|x\|)$, $T_x = \{\xi \in \mathbb{S}^2 : \xi \perp x\}$, $c(\lambda)^{-1} = \lambda^{-2}\omega_1\alpha_0(T)$, and Δ is Laplace-Beltrami operator.

In addition, we focus on the computing procedure for the evaluation of the relative efficiency by using spherical data on the 2-dimensional unit sphere. Finally, a short discussion related to comparing the relative efficiency is made.

2. Numerical Study for Evaluating the ARE

The relative efficiency of the kernel estimator (1.1) to those of the estimator (1.8) is of good interest. Using the results of Lemmas in Appendix, the relative efficiencies of the estimator (1.1) to those of the estimator (1.8) are immediate. Hence we omit the proof of Theorem 1. See Lemmas in Appendix. To make the numerical illustration of the relative efficiencies between these estimators, we introduce an example on $\mathbb{S}^2$ to evaluate the values of the constants.

2.1. Simulation procedure

For computing of ARE (1.9), finite sample sizes, $n = 10, 30, 50, 70, 100, 300$, and 1000 are investigated as follows. The most widely referred distribution for directional data is the von Mises-Fisher distribution such that

$$f(s, \phi) = \frac{\kappa}{2\pi \sinh \kappa} \exp\left[\kappa(\sin s \sin\alpha \cos(\phi - \beta) + \cos s \cos\alpha)\right],$$

where $0 \le s < \pi$, $0 \le \phi < 2\pi$. There are three parameters α, β, and κ. We generate pseudo-random variates from the von Mises-Fisher distribution with parameters vMF(α, β, κ) as suggested in Fisher *et al.* (1993, p.59). Given the random variables (X, Y) and angle $\Phi \in [0, \pi)$ with an Uniform distribution, the curve through (X, Y) is determined by Φ and $S = X\cos\Phi + Y\sin\Phi$.

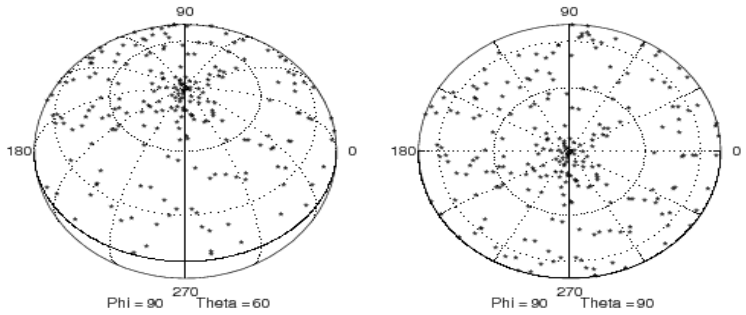

Figure 1: *Plotting for the spherical data points on the surface of* $\mathbb{S}^2$

We provide here a brief discussion of the computation for the four constants in Theorem 1. We first start by assuming that the generated points occur according to the distribution f. The kernel used in simulation procedure is $T(v) = e^{-<v,v>^{1/2}}$; $-\infty < v < \infty$. Using the kernel and the four constants discussed in Theorem 1, we compute the value of ARE (1.9). These integrals are approximated by use of numerical integration. We consider that any point $\mathbb{S}^2$ can be parameterized by $x(\theta, \phi) = (\sin\theta\cos\phi, \sin\theta\sin\phi, \cos\theta)$, $\theta \in [0, \pi)$, $\phi \in [0, 2\pi)$ and find vector points on tangent space. We can choose a large number N instead of infinity, and use the geodesic spherical coordinates, given by $y(t, \xi) = \exp_p(t\xi)$ for computing C_1 and C_2. Then we have that

$$\int_{\mathbb{S}^2} (\Delta f(p))^2 dV_g(p) = \int_{\mathcal{E}_p} \int_{(-1,1)} D_\xi^2 f(y(hs, \xi)) ds d\mu_p(\xi), \tag{2.1}$$

where $\mathcal{E}_p = \{\xi \in T_p(\mathbb{S}^2) | |\xi| = 1\}$. Details are in Park (2012, Appendix A.1 and Lemma A.1–A.2). Algorithm flows for the computation of the ARE are created in the following way.

1. Generate an data point (X, Y) and Φ from Uniform distribution such that $X \sim U(-\pi, \pi)$, $Y \sim U(0, \pi)$, and $\Phi \sim U(0, 2\pi)$, and take a surface data (S, Φ).

2. Build the tangent vector v_i, corresponding to the data point $x_i = (s_i, \phi_i)$, $i = 1, \ldots, n$ using by (1.5) for any $p \in \mathbb{S}^2$.

3. Compute the four constants C_1, C_2, D_1, and D_2.

4. Define a kernel function on the tangent space and choose the optimal smoothing parameters $h_{AMISE} = (fC_1/(nC_2))^{1/3}$ that minimizes the Asymptotic Mean Integrated Square Error (AMISE) from Lemma 1 in Appendix, where C_1 and C_2 are in (1.10).

5. Substituting the optimal smoothing parameter into AMISE($\hat{f}_n$), and compute the constants of (1.9).

The above algorithm is implemented in **R** environment system in the CRAN (http://cran.R-project.org) while others will be approximated by use of numerical integration where MATLAB-program proceeds.

2.2. Spherical data

Observations on normals to the orbital planes of long-period comets with sample sizes $n = 240$ are from Fisher *et al.* (1993, pp. 160–161). Figure 1 shows a display of the data to 240 cometary orbits, which are only dispersed on the upper hemisphere (see Bowman and Azzalini, 1997, pp. 12–14).

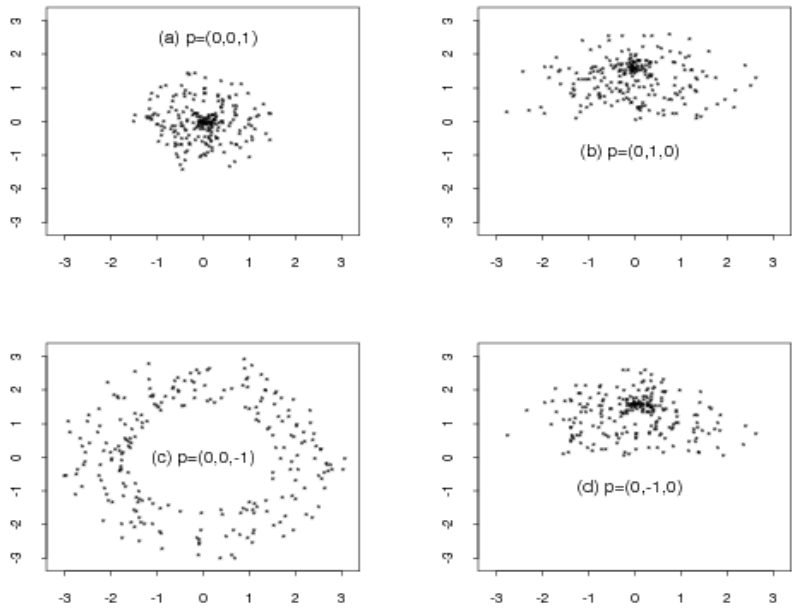

Figure 2: *Plotting for the vector points on the tangent space $T_p(\mathbb{S}^2)$. Plot on (a), (b), (c) and (d) are the tangent vectors v when $p = (0, 0, 1)$, $p = (0, 1, 0)$, $p = (0, 0, -1)$ and $p = (0, -1, 0)$, respectively.*

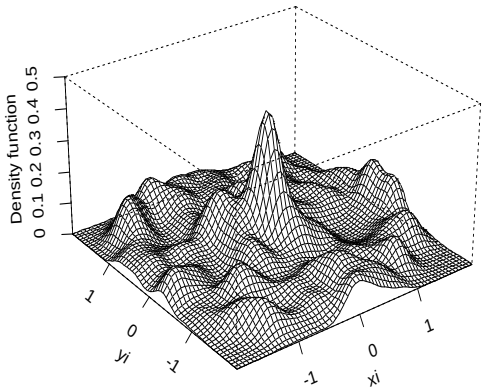

Figure 3: *Perspective plot for the spherical data. Vertical axis is proportional to $\hat{f}$, discs in horizontal plane represent the equal-area projection of the unit sphere.*

For each comet, the observations are measured as the angle of latitude and longitude. "Theta" and "Phi" denoted in Figure 1 are the vertical and horizontal rotation of the displayed sphere, respectively. For given data point x_i, $i = 1, \ldots, 240$, we can find the tangent vectors v_i corresponding to x_i by using (1.4) for each $p \in \mathbb{S}^2$. Figure 2 shows a display of the tangent vector points v_i, $i = 1, \ldots, 240$, on the tangent space, for example $p = (0, 0, 1)$, $p = (0, 1, 0)$, $p = (0, 0, -1)$ and $p = (0, 0, -1)$, respectively.

We employ the estimator $\hat{f}_n(p)$ with the kernel $K(v) = e^{-v}$ for $v \in T_p(\mathbb{S}^2)$. The smoothing parameter formula used in this spherical data is given by $h = \min_h \text{AMISE}(\hat{f}_n) = (fC_1/(nC_2))^{1/3}$. Figure 3 depicts the perspective plot. For visualization we use an equal-area projection method of the unit sphere into a disc of radius 2 (see Watson, 1983, p.21).

Table 1: The AREs from the kernel estimator $\hat{f}_n$ over $\hat{g}_n$ using the kernel e^{-t} with the sample sizes $n = 10, 30, 50, 70, 100, 300, 1000$ and with given the parameter vMF(0.02, 0.13, 1.35).

Sample size n	ARE($\hat{g}_n$; $\hat{f}_n$)	vMF($\hat{\alpha}$, $\hat{\beta}$, $\hat{\kappa}$)
10	2.987067	(0.963, 1.761, 5.482)
30	1.236650	(0.241, 0.911, 2.140)
50	1.076593	(0.117, 0.346, 1.891)
70	1.019220	(0.089, 0.294, 1.806)
100	1.002381	(0.042, 0.174, 1.474)
300	1.000298	(0.026, 0.137, 1.361)
1000	1.000017	(0.020, 0.131, 1.352)

3. Conclusion

We present the point of assessing the adequacy of fit of this distribution to the spherical data. First, since we show the graphical display which permit a general assessment of the plausibility of the distribution from Figure 3, the next step comprises a significance test companion to the graphical procedures (*i.e.* Q-Q plots). A restriction on the use of these methods is that they are based on approximations which are only valid if κ exceeds 5. However, in many data, κ will not have such a high value. With the references Fisher *et al.* (1993), Section 5.3.2(p.129) and Dhillon and Sra (2003), Section 5.2, we deal with estimating parameters of the vMF(α, β, κ) distribution. The results are summarized in Table 1 according to the random samples with given $\hat{\alpha} = 0.02$, $\hat{\beta} = 0.14$, $\hat{\kappa} = 1.35$, which are given by using an EM-algorithm that proceeds by iterative updates to estimate the parameters of the vMF distribution on the orbital comets data. Details for the parameter estimation are in Fisher *et al.* (1993), pp. 129–131, and Dhillon and Sra (2003), Table 1 in Section 5.2.1. Thereby since $\hat{\kappa} < 5$, we have the value of test statistics $R = 0.712$ for mean direction using the percentage points of test criterion statistics for the vMF distribution in Fisher *et al.*, Appendix A, p.266. So, for test of $\kappa = \kappa_0$ against $\kappa \neq \kappa_0$, the significane probability is about 5% and there are some grounds to accepte the null hypothesis.

The simulation result is given by the following Table, respectively. The resulting values of C_1, C_2, D_1, and D_2 are substituted in the equation for the ARE in (1.9). The ARE values are tabulated in Table 1. From the results with the kernel e^{-t}, we see that the ARE($\hat{g}_n$; $\hat{f}_n$) converges to 1. It is clear from the ARE of (1.9) that $\lim_{n\to\infty}$ ARE $\to 1$ for the kernels. Besides, according to the first term of the bias in Lemma 1 of Appendix, we can find that the estimator $\hat{f}_n(p)$ is asymptotically unbiased as $h \to 0$.

Recently, the statistical methods by using geometric specifications of a space (*i.e.* Lie group) have been used for image processing (for example, astrophysics, Mean Shift Techniques and Coordinate Measuring Machine). See Fletcher *et al.* (2003) and Kim and Park (2012). The comparison of the ARE of the estimators employed in this paper is motivated by the applications of those. Therefore we show that the relative efficiencies of the kernel estimator is useful when comparing those of the existing estimator (1.8). Although real data with which to demonstrate the ARE is unavailable to us at nonparametric approaches, our example for simulation data would be of significant benefit in practice.

Appendix: Asymptotic Behavior of the Bias and Variance

We describe the asymptotic formula of the bias and variance of the kernel estimator defined by (1.1) of the Introduction, which have been proposed by Park (2012). From (A.3) and (A.4), note that the asymptotic rate of convergence for the bias and variance of $\hat{g}_n(x)$ in Lemma 2 is analogous to that of Lemma 1. While the sectional curvature κ cannot be found in Lemma 2, the result of Lemma 1

contains it. Noted that various geometric information (*i.e.* components of curvature tensor or covariant derivatives) will occur in asymptotic expansions of the proposed kernel density estimator according to another geometric structure of a space.

Lemma 1. *Assume that the unknown density f is bounded and continuously four times differentiable. Then we have the bias and variance of the proposed kernel estimator for $\kappa = 1$ as follows:*

$$\begin{aligned} Bias\left(\hat{f}_n(p)\right) &= \frac{Vol(\mathcal{E}_p)}{4}\Delta f(p)\int_0^\infty T(s)s^3ds\frac{h^2}{C_h} \\ &+ \left[\frac{Vol(\mathcal{E}_p)}{192}\left\{-4\kappa\Delta f(p) + 3\sum_{i,j=1}^{2}\nabla^4_{ijij}f(p)\right\}\times\int_0^\infty T(s)s^5ds\right]\frac{h^4}{C_h} \\ &+ o\left(\frac{h^4}{C_h}\right) \quad as\ \ h\to 0, \end{aligned} \tag{A.1}$$

$$\begin{aligned} Var\left(\hat{f}_n(p)\right) &= \frac{Vol(\mathcal{E}_p)}{nh^2}\left[\int_0^\infty T^2(s)sdsf(p) + \left\{\frac{1}{4}\left(\Delta f(p) - 2\kappa\frac{1}{3}f(p)\right)\int_0^\infty T^2(s)s^3ds\right\}\frac{h^2}{C_h^2}\right. \\ &\left. + \frac{1}{192}\left\{\frac{190}{15}\kappa^2 f(p) - 4\kappa\Delta f(p) + 3\sum_{i,j=1}^{2}\nabla^4_{ijij}f(p)\right\}\frac{h^4}{C_h^2}\times\int_0^\infty T^2(s)s^5ds\right] - \frac{1}{n}f^2(p) \\ &- \frac{1}{n}\left\{\frac{Vol(\mathcal{E}_p)}{2}f(p)\Delta f(p)\int_0^\infty T^2(s)s^3ds\right\}\frac{h^2}{C_h} \\ &+ o\left(\left(nC_h^2h^{-2}\right)^{-1} + \left(nC_hh^{-2}\right)^{-1}\right) \quad as\ \ nh^2\to\infty, h\to 0, \end{aligned} \tag{A.2}$$

where Δ is Laplace-Beltrami operator, and $\nabla^4_{ijij}f(p) = \partial^4/(\partial x^i\partial x^j\partial x^i\partial x^j)\,f(p)$.

For comparing the behaviors of the bias and variance in Lemma 1, we give the asymptotic expansions of the bias and variance of $\hat{g}_n(x)$ in the following lemma.

Lemma 2. *Assume that all derivatives of g are well defined and continuous. For random variables $X_1, X_2, \ldots, X_n$ taking values on m-dimensional unit sphere, we have the asymptotic behavior of bias and variance of kernel estimator (1.8) as follows:*

$$\begin{aligned} Bias\left(\hat{g}_n(x)\right) &= \frac{\lambda^{-2}}{2\alpha_0(T)}\int_{T_x}D^2_\xi\overline{g}(x)d\mu_1(\xi)\int_0^\infty T(s)s^3ds \\ &+ \frac{\lambda^{-4}}{24\alpha_0(T)}\left\{-\frac{22}{30}\int_{T_x}D^2_\xi\overline{g}(x)d\mu_1(\xi) + \frac{1}{3}\int_{T_x}D^4_\xi\overline{g}(x)d\mu_1(\xi)\right\}\times\int_0^\infty T(s)s^5ds \\ &+ o\left(\frac{\lambda^{-4}}{\alpha_0(T)}\right),\ \ as\ \ \lambda\to\infty, \end{aligned} \tag{A.3}$$

$$\begin{aligned} Var\left(\hat{g}_n(x)\right) &= \frac{\lambda^2\omega_1}{n}\left[\frac{1}{c(\lambda)^{-2}}\int_0^\infty T^2(s)sds\cdot g(x) + \frac{c(\lambda)^2}{\lambda^2}\left\{\int_{T_x}D^2_\xi\overline{g}(x)d\mu_1(\xi) - \frac{1}{2}g(x)\right\}\int_0^\infty T^2(s)s^3ds\right. \\ &+ \frac{c(\lambda)^2}{\lambda^4}\left\{\frac{1}{3}\int_{T_x}D^2_\xi\overline{g}(x)d\mu_1(\xi) + \int_{T_x}D^4_\xi\overline{g}(x)d\mu_1(\xi)\right. \\ &\left.\left. - \frac{22}{(24\times 30)}\int_{T_x}D^2_\xi\overline{g}(x)d\mu_1(\xi)\cdot g(x)\right\}\int_0^\infty T^2(s)s^5ds\right] - \frac{1}{n}g^2(x) \end{aligned}$$

$$-\frac{\omega_1 c(\lambda)}{n\lambda^2}\left\{g(x)\int_{T_x} D_\xi^2 \overline{g}(x)d\mu_1(\xi)\int_0^\infty T^2(s)s^3 ds\right\} + o\left(\frac{c(\lambda)^2}{n\lambda^2}+\frac{c(\lambda)}{n\lambda^2}\right),$$
$$as\ \ n\lambda^2\to\infty,\ \lambda\to\infty, \tag{A.4}$$

where $\alpha_0(T)=\int_0^\infty T(s)sds$, $D_\xi^s g = D_\xi D_\xi^{s-1} g$, $\overline{g}(x)=g(x/\|x\|)$, $T_x=\{\xi\in\mathbb{S}^2 : \xi\perp x\}$, $c(\lambda)^{-1}=\lambda^{-2}\omega_1\alpha_0(T)$, *and* $\omega_1=\mu_1(\mathbb{S}^2)$, *where* μ_1 *is a Lebesgue measure of the unit sphere.*

Acknowledgements

The author would like to thank the referees for their careful reading of the manuscript and their constructive comments and thank the Editor in Chief and the Associate Editor for their careful work.

References

Bai, Z. D., Rao, C. R. and Zaho, L. C. (1988). Kernel estimators of density function of directional data, *Journal of Multivariate Analysis*, **27**, 24–39.

Bowman, A. W. and Azzalini, A. (1997). *Applied Smoothing Techniques for Data Analysis*, Clarendon press, Oxford.

Dhillon, I. S. and Sra, S. (2003). Modeling data using directional distributions, *Technical Report No. TR-03-06*, The University of Texas at Austin.

Fisher, N. I., Lewis, T. and Embleton, B. J. (1993). *Statistical Analysis of Spherical Data*, Cambridge, Cambridge University Press, England.

Fletcher, P., Lu, C. and Joshi, S. (2003). Statistics of shape via principal geodesic analysis on lie groups, In *Proceedings of the IEEE Conference* on Computer Vision and Pattern Recognition, Madison, WI, **1**, 95–101.

Hall, P., Watson, G. and Cabrera, J. (1987). Kernel density estimation with spherical data, *Biometrika*, **74**, 751–762.

Kim, Y. T. and Park, H. S. (2012). Geometric structures arising from kernel density estimation on Riemannian manifolds, *Journal of Multivariate Analysis*, **114**, 112–126.

Park, H. S. (2012). Asymptotic behavior of the kernel density estimator from a geometric viewpoint, *Communications in Statistics - Theory and Methods*, **41**, 3479–3496.

Watson, G. S. (1983). *Statistics on Spheres*, Wiley, New York.

Received August 3, 2012; Revised December 7, 2012; Accepted January 10, 2013